Degradation of the charge collection efficiency of an n-type Fz silicon diode subjected to MeV proton irradiation

(Article begins on next page)

28 April 2024

Micro-IBA analysis of Au/Si eutectic "crop-circles"

Giampiero Amato[1], Alfio Battiato[2], Luca Croin[1,3], Milko Jaksic[4], Zdravko Siketic[4], Umberto Vignolo[2], Ettore Vittone[2*]

[1] The Quantum Research Lab, INRiM, Strada delle Cacce 91, 10135 Torino, Italy

[2] Physics Department, NIS Research Centre and CNISM, University of Torino, via P. Giuria 1, 10125 Torino, Italy.

[3] Dept. of Applied Science and Technology, Politecnico di Torino, Corso Duca degli Abruzzi 24, 10129 Torino, Italy

[2] Department for Experimental Physics, Ruđer Bošković Institute, P.O.Box 180, 10002 Zagreb, Croatia.

Abstract

When a thin gold layer is deposited onto the native oxide of a silicon wafer and is annealed at temperatures greater than 600°C, peculiar circular features, few micrometers in diameter, with a regular polygon at the centre of each circle, reminiscent of so called "alien" crop circles, can be observed.

A model has been recently proposed in [1], where the formation of such circular structures is attributed to the interdiffusion of gold and silicon through holes in the native oxide induced by the weakening of the amorphous silica matrix occurring during the annealing process. The rupture of the liquid Au/Si eutectic disc surrounding the pinhole in the oxide causes the debris to be pulled to the edges of the disk, forming Au droplets around it and leaving an empty zone of bare silicon oxide.

In this paper, we present a morphological study and a RBS/PIXE analyses of these circular structures, carried out by scanning electron microscopy and by 4 MeV C microbeam, respectively. The results confirm the depletion of gold in the denuded circular zones, and the presence of gold droplets in the centres, which can be attributed to the Au segregation occurring during the cooling stage.

1 Introduction

---

* Corresponding author: ettore.vittone@unito.it

Solid-state dewetting of metallic thin films during annealing is a well-known phenomenon occurring by thermally activation of atomic diffusion and driven by interface film/surface energy minimization lowering. It consists in the agglomeration of the film during annealing, forming holes and droplets, randomly distributed through the film substrate. These metallic droplets can catalyse the growth of nanostructures to be used for numerous applications ranging from bio sensors to photonic devices [2][3] .

One of the prerequisites for metallic thin film dewetting, is the presence of a diffusion barrier, which isolates the metal film from the substrate. If the substrate is silicon, CVD or thermally grown oxide effectively prevent any interdiffusion. However, if the barrier is given by a thin native oxide layer, the weakening of the amorphous matrix induced by the annealing process, causes the opening of pinholes, through which the metal can effectively diffuse into the silicon substrate, forming an eutectic layer, which spreads around the pinhole.

This is what we experienced during the deposition of thin (few tens of nanometers) Au film on silicon substrates, with nanometer thick oxide layers, annealed at temperatures greater than 600°C. We observed peculiar circular features, surrounded by gold droplets and with a regular polygon at the centre of each circle, whose shape depends on the orientation of the substrate.

In a recent paper [1], a systematic investigation on the role of the annealing temperature and of the Au layer thickness allowed the formation mechanism of these circular nano-structures to be properly modelled: the opening of narrow channels in the native oxide induces the formation of a liquid AuSi eutectic layer with a thickness determined by the thickness of the deposited Au film. The central polygons occur in correspondence of the oxide channel openings and represent regions filled with a AuSi alloy which, during cooling, segregated into pure Au and Si. Their typical dimensions vary in the range of few micrometers and are related to the diameters of the circles, which extend up to few tens of micrometers.

In this paper, we report on a morphological investigation, which provides results in excellent agreement with those reported in [1] and extend the analysis to a differently oriented substrate. Moreover, since, to our knowledge, no elemental distribution analyses of these "crop circles" have been reported so-far, we report on micro ion beam analysescarried out at the Ruder Boskovic Institute of Zagreb, ito image the composition of the disks and of the Au central regular structure.

2. Experimental

The silicon substrates used in this work were B doped, and (100) or (111) –oriented. Silicon wafers were diced into 1×1 cm^2 squares and cleaned in a class 100 clean room by sonication in acetone and isopropyl alcohol, rinsed in deionized water and dried with nitrogen flow. After this treatment, the substrates presented a native oxide layer with a thickness of 2 nm, as estimated by measurements performed with a J.A. Woollam alpha-SE spectroscopic ellipsometer.

Thin (15-100 nm) gold films were then deposited (rate of the order of 1-2 nm/min) by thermal evaporation from a commercial effusion cell in high vacuum (less than 10^{-6} Pa) conditions.

After the gold deposition on the oxide/silicon substrate, the samples were inserted in a Jipelec JetFirst 100C rapid thermal processing system [4], kept at a pressure of 0.1 Pa, annealed by an array of 12 halogen lamps, kept at the process temperature (ranging from 600 to 800°C) for 5-15 min and rapidly cooled back to room temperature .

A focused ns-pulsed Nd:YAG laser was used to mark some processed samples, in order to easily individuate regions of interest, to be morphologically characterized by optical and electron microscopy and by Ion Beam Analysis (IBA) techniques.

The scanning electron microscope was an Inspect F SEM-FEG (Field Emission Gun) from FEI company, with a beam diameter of 3 nm. The SEM micrographs were analyzed with the open source image processing package, ImageJ [5].

Particle Induced X-ray Emission (PIXE) and Rutherford Backscattering Spectroscopy (RBS) analyses were performed at the ion microbeam facility of the Ruder Boskovic Institute in Zagreb [6]. The samples were mounted on an electrically grounded Al frame, fixed with conductive silver paste and positioned inside the vacuum chamber (P<10-5 Pa). The 4 MeV C3+ beam, coming from the HVEE 1.0 MV Tandetron accelerator, was focused down to a 3 µm spot size by the triplet of the Oxford Microbeam and Melburne lenses and raster scanned over the sample. Ion currents, measured by means of a standard current integrator and a counter, were of the order of 10 pA.

PIXE spectra were collected by a Si(Li) detector with a resolution of 150 eV (at 5.9 keV) and a nominal area of 30 mm2, equipped with a 25 µm thick Be window, positioned at an angle of 135° with respect to the incoming ion beam. Rutherford backscattering spectra were measured by an Annular Si detector ORTEC TC-030-450-300-S (12 mm central hole, 450 mm2 active area, 100 µm depletion depth) positioned 35 mm from the sample. Analog signals from the detectors were simultaneously

collected through conventional spectroscopy chains connected to the multiparameter acquisition system SPECTOR [7].

3. Results and discussion

Fig. 1 shows the morphology of a 35 nm thick gold film before and after the thermal treatment at 600°C for 7 min. The as deposited film shows a micro/nanocrystalline structure continuously covering the entire substrate (Fig. 1a); after annealing, the continuous film decomposes into isolated micro/nano gold droplets. The lowering of the (thin-film/substrate) interfacial energy drives this dewetting process and it typically occurs via surface diffusion in the solid state because the annealing temperature is well below the Au melting point [8]. If deposited onto a uniform, 280 nm thick, thermally grown silicon oxide layer, the gold droplets are randomly distributed (Fig. 1c); however, if deposited on the native thin oxide layer, peculiar circular features can be observed, with regular structures located in the centre, surrounded by irregulars blisters (Fg. 1b). According to the model of T. S. Matthews et al. [1], if the silicon oxide layer remains intact, as in the case of 280 nm thick oxide layer in Fig. 1c, it acts as a barrier, which prevents the pure silicon from mixing with gold and then allowing the formation of randomly distributed gold droplets.

In the case of thin native oxide layer, the annealing process induces a weakening of the oxide structure and the formation of pinholes, through which silicon and gold interdiffuse, forming a layer of eutectic $Au_{0.81}/Si_{0.19}$ alloy with nearly the same thickness as the original gold. Being the process temperature (600°C) higher than the eutectic melting point (363°C), the alloy is liquid and spreads in a virtually perfect circle from the central pinhole. When the eutectic discs achieve critical diameters, the high surface energy of the Au/Si liquid alloy induces the rupture of the eutectic layer, and debris are pulled to the edges of the disks, forming droplets around it and leaving an empty, or denuded, zone (DZ) of bare silicon oxide. During cooling, gold and silicon located in the central zone segregate; silicon is drained towards the substrate reservoir and gold accumulates in the centre of the denuded circular zone. The side views schematics in Fig. 2 outlines the three phases of the Au/Si "crop circles" formation.

The segregation of gold occurs in regular structures with shapes depending on the silicon substrate orientation: squares if (100) oriented and equilateral triangles if (111) oriented (Fig. 3). In the former case, transmission electron microscopy analysis reported in [1] reveals that surface squares are the bases of inverted pyramids embedded in the silicon wafer with the four triangular sides lying along the

(111) atomic planes. From mass conservation law and considering the correct geometrical parameters, the model provides the relation

$$(1) \qquad R = a^{3/2} \cdot \sqrt{\frac{1}{3\pi\sqrt{2}} \frac{f}{(1-f)} \cdot \frac{V_{Au}}{V_{Si}} \cdot \frac{1}{d}}$$

where R is the radius of the DZ, a the side length of the central square, d is the Au film thickness and f is the Au/Si molar fraction and V_{Au}, V_{Si} are the molar volumes of gold and silicon, respectively.

In order to validate this model, we have measured DZ radii and size lengths of the central squares of XXX eutectic disks formed from Au thin films of 35, 50, 110 nm thickness. Fig. 3b shows a clear linear trend of R vs. $a^{3/2}$; by plotting the slopes of the linear fits vs. $1/\sqrt{d}$, a molar fraction f=(0.80±0.01) of Au in the Au/Si was extracted from eq. (1), in excellent agreement with the model and the experimental data reported by Matthews et al. [1].

In order to complete the validation of the model, we carried out a microPIXE and microRBS analysis of circular structures in order to map the elemental distribution of gold. The sample results from the annealing at 600°C for 7 minutes of 50 nm gold layer deposited on the native oxide of a (100) oriented silicon substrate.

The 4.0 MeV C^{3+} ion probe was chosen because the shallow penetration in silicon (4 μm) and in gold (1.5 μm) and the small straggling (0.2 and 0.3 μm, respectively) were supposed to be suitable to investigate the gold "crop circles" both in the denude zone and in the central region [9].

Fig.4 summarizes the procedure and the results of the IBA analysis. "Crop circles" were localized in the SEM image through laser markers (Fig. 4a,b). The ion microbeam raster scanned the 75x75 μm^2 region including a "crop circle", ~45 μm in diameter, with two gold segregation centers. RBS/PIXE signals were simultaneously acquired in order to generate Au maps extracted from the higher energy backscattered ions and Au M_α characteristic peaks (Fig. 4k,h), respectively. As it is apparent from both the maps, gold droplets surround the circular denuded zone and two Au segregation centers are detected in the center of the circle.

The PIXE spectrum relevant to a small region in the denuded zone (Fig. 4f) shows a drastic decrease of the gold signal, confirming the rupture of the Au/Si eutectic layer. Similar conclusions can be drawn from the RBS spectrum (Fig. 4g). In this latter spectrum, signals relevant to gold scattering atoms appear at high energy. However, these very sporadic counts do not provide a clear evidence of presence

of a thin gold layer in the denuded zone; in fact, they can originate from debris observable in the high magnification SEM image in Fig. 4c and/or by the microbeam halo and can be actually signals from the thick gold layer aside. Moreover, SIMNRA [10] simulations reveal that if a thin (~1nm) gold layer were still present in the denuded zone, the small terminal peak at channel 780 should be at least one order of magnitude higher than observed in fig. 4g, as compared to the silicon signal.

4. Conclusions

This paper describes the analysis of the dewetting of Au thin films deposited on silicon with in presence of a thin native oxide layer. After annealing at temperature higher than 600°C, hundreds empty circular structures surrounded by Au droplets and with a regular polygon (a square if the substrate is (100) oriented, a triangle if (111) oriented) in the centre of each circle, have been morphologically analyzed in order to evaluate the relationship between the size of the central square, the diameter of the denuded circle, and the thin film thickness. The results are in excellent agreement with the model presented in [1], which attribute the formation of these structures to the rupture of the Au/Si liquid eutectic layer. Micro PIXE and RBS analyses carried out using 4 MeV carbon microbeam confirm the dominant presence of Au in the central segregation point. The circular zone is, within the experimental sensitivity, almost denuded of gold, which, during the eutectic liquid rupture, aggregates to the droplets surrounding the disk or segregates in the central Au regular structure.

References

[1]   T. S. Matthews, C. Sawyer, D. F. Ogletree, Z. Liliental-Weber, D. C. Chrzan, J. Wu, Phys. Rev. Lett. **108** (2012) 096102.

[2]   D. Kim, A. L. Giermann, C. V. Thompson, Applied Physics Letters 95 (2009) 251903,.

[3]   N.D. Zakharov, P. Werner, G. Gerth, L. Schubert, L. Sokolov, U. Gösele, Journal of Crystal Growth **290** (2006) 6–10,.

[4]   Marco Piazzi, Luca Croin, Ettore Vittone, Giampiero Amato, SpringerPlus **1** (2012) 52,.

[5]   C.A. Schneider, W.S. Rasband, K.W. Eliceiri, Nature Methods **9** (2012) 671–5.

[6]   M. Jaksic, I. Bogdanovic-Radovic, M. Bogovac, V. Desnica, S. Fazinic, M. Karlusic, Z. Medunic, H. Muto, Z. Pastuovic, Z. Siketic, N. Skukan, T Tadic, Nucl. Instr. and Meth. in Phys. Res. B, .**260**, 114.

[7] M. Bogovac, I. Bogdanović, S. Fazinić, M. Jakšić, L. Kukec, W. Wilhelm, Nucl. Instr. and Meth. B 89 (1994) , 219.

[8] Donghyun Kim, Amanda L. Giermann, Carl V. Thompson, Applied Physics Letters **95** (2009) 251903.

[9] See www.SRIM.org

[10] M. Mayer, SIMNRA User's Guide, Report IPP 9/113, Max-Planck-Institut für Plasmaphysik, Garching, Germany, 1997, http://home.rzg.mpg.de/~mam/index.html

Figure Captions

Fig. 1: Scanning electron microscopy (SEM) images of the 35 nm thick gold thin layer as deposited onto a native silicon oxide layer (a) and (b) after annealing at 600°C; (c) similar as (b), but relevant to gold deposition on a thermally grown silicon oxide layer, 280 nm thick.

Fig. 2: A side-view schematic of the as deposited structure (I). When a pinhole in the native silicon oxide layer is formed during annealing, the Au/Si eutectic layer spreads around the central pinhole (II). After the eutectic layer rupture and the subsequent cooling (III), a gold regular structure (of size a) is segregated in the centre and gold droplets surround the denuded circle of radius R.

Fig. 3: (a) SEM image of "crop circles" on (100) silicon substrates; lines demonstrates that the square bases of the inverted pyramids are oriented along the crystal planes. (b) DZ radii (R) vs. size length (a) of the central squares raised to the power of 3/2 relevant to Au films of different thicknesses. The lines refer to linear fit relevant to different thin film thicknesses. (c) same as in (a) but relevant to (111) silicon substrates; gold aggregate in oriented triangular structures in the centres of the DZ.

Fig. 4: (a,b,c) SEM images at different magnifications of the region under analysis identified with a laser marker (M); (d) RBS map of the ROI highlighted by the rectangle of the spectrum shown in k) and relevant to the SEM image b); (e) PIXE map of the Au Mα peak highlighted by the rectangle of the spectrum shown in h) and relevant to the SEM image b); (g) RBS and (f) PIXE spectra of the denuded zone.
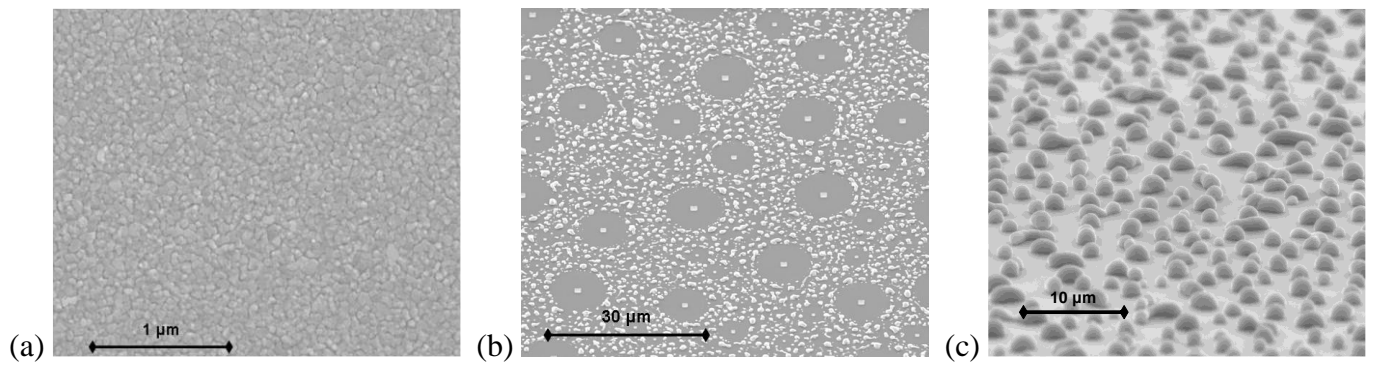
Fig. 1: Scanning electron microscopy (SEM) images of the 35 nm thick gold thin layer as deposited onto a native silicon oxide layer (a) and (b) after annealing at 600°C; (c) similar as (b), but relevant to gold deposition on a thermally grown silicon oxide layer, 280 nm thick.
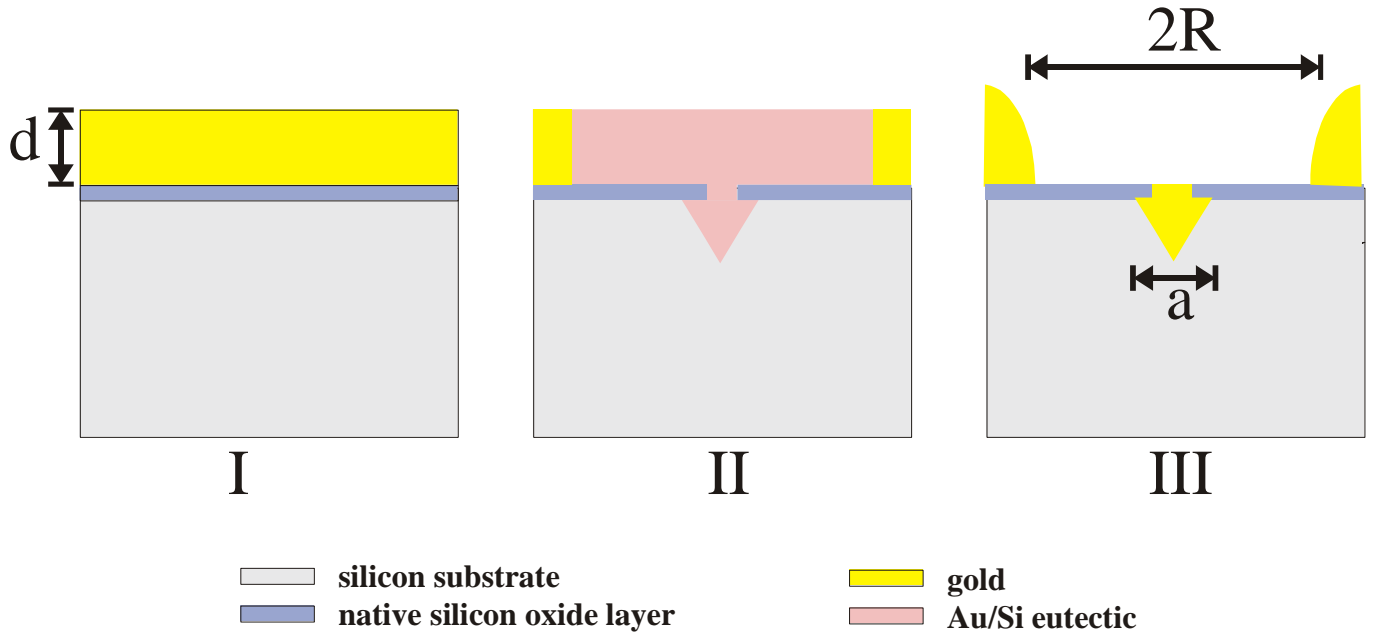
Fig. 2: A side-view schematic of the as deposited structure (I). When a pinhole in the native silicon oxide layer is formed during annealing, the Au/Si eutectic layer spreads around the central pinhole (II). After the eutectic layer rupture and the subsequent cooling (III), a gold regular structure (of size a) is segregated in the centre and gold droplets surround the denuded circle of radius R.
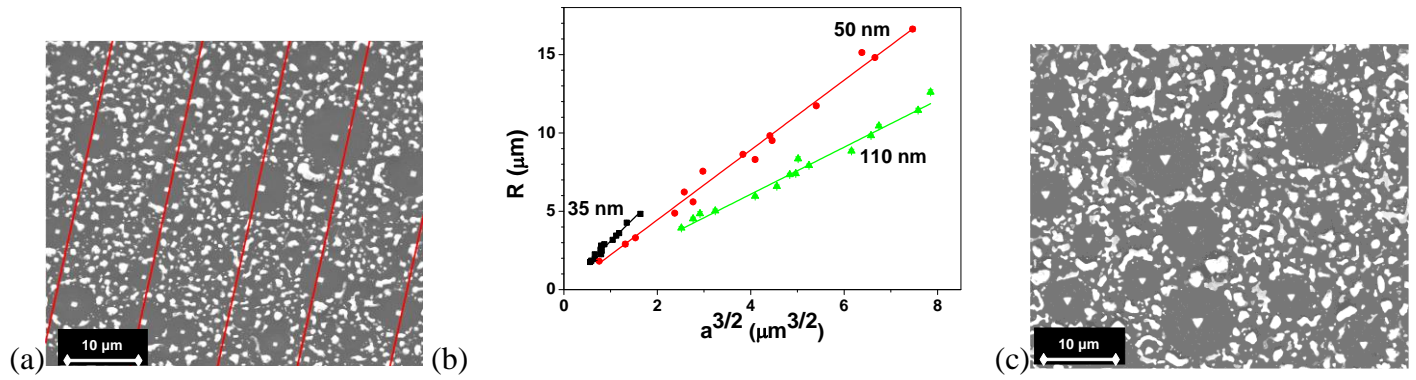
Fig. 3: (a) SEM image of "crop circles" on (100) silicon substrates; lines demonstrates that the square bases of the inverted pyramids are oriented along the crystal planes. (b) DZ radii (R) vs. size length (a) of the central squares raised to the power of 3/2 relevant to Au films of different thicknesses. The lines refer to linear fit relevant to different thin film thicknesses. (c) same as in (a) but relevant to (111) silicon substrates; gold aggregate in oriented triangular structures in the centres of the DZ.
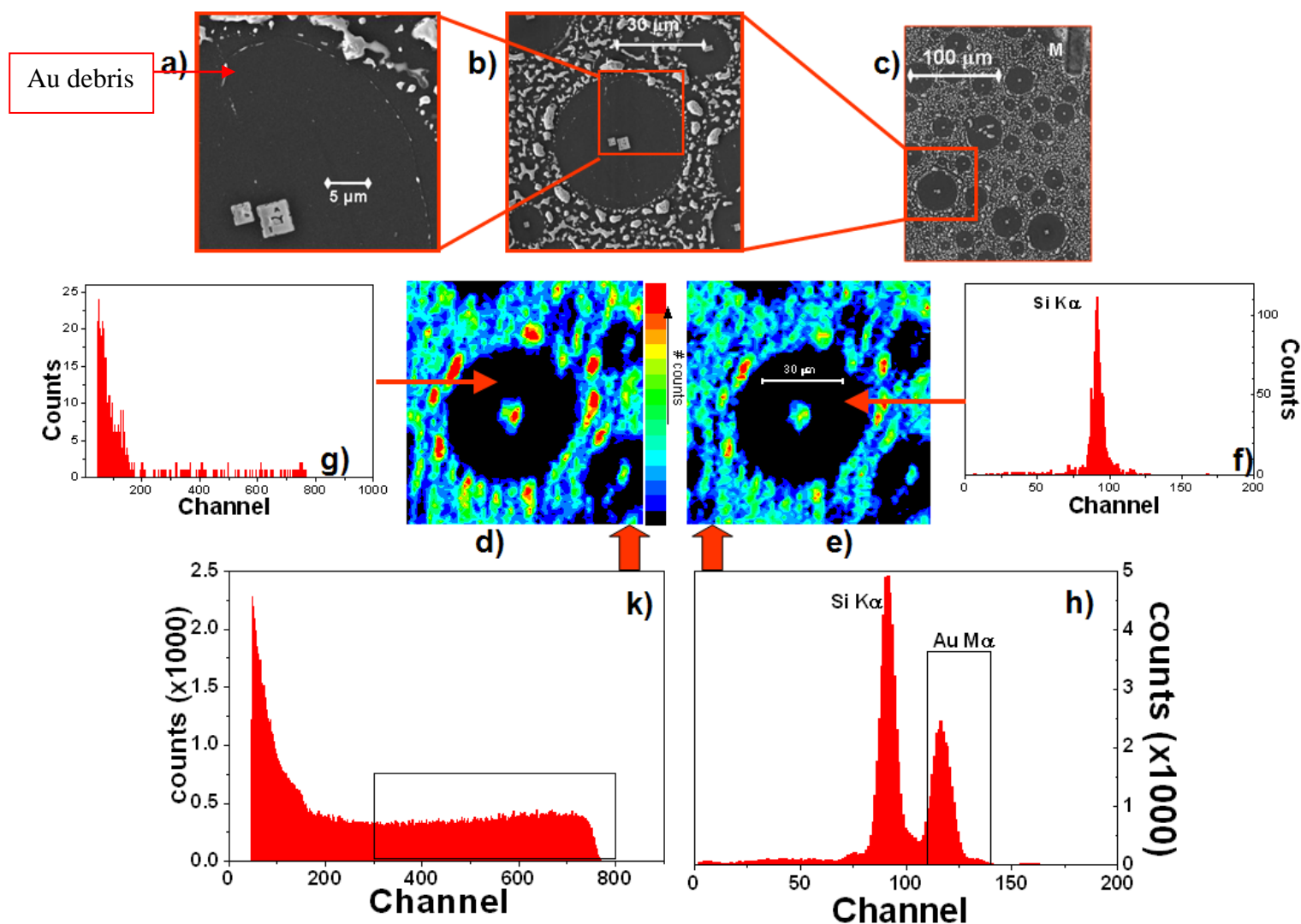
Fig. 4: (a,b,c) SEM images at different magnifications of the region under analysis identified with a laser marker (M); (d) RBS map of the ROI highlighted by the rectangle of the spectrum shown in k) and relevant to the SEM image b); (e) PIXE map of the Au Mα peak highlighted by the rectangle of the spectrum shown in h) and relevant to the SEM image b); (g) RBS and (f) PIXE spectra of the denuded zone.